Title: Polygenic barriers to sex chromosome turnover

Author: Pavitra Muralidhar

Department of Ecology & Evolution, University of Chicago
pmuralidhar@uchicago.edu

In organisms with distinct sexes, sex is commonly determined by segregation of a pair of chromosomes in paternal meiosis (male heterogamety) or maternal meiosis (female heterogamety). Evolutionary transitions between sex-chromosome systems—which change the chromosome pair that determines sex, the system of heterogamety, or both—are frequent in some clades. In others, however, sex chromosome systems show long-term stability. Previous explanations of this stasis rely on evolutionary dynamics peculiar to sex linkage, such as the accumulation of deleterious mutations on the sex-specific chromosome or sexually antagonistic mutations on either sex chromosome. Here, I show that the ordinary operation of stabilizing selection on quantitative traits can, as a by-product, promote stability of sex chromosome systems. The reason is that stabilizing selection on a trait permits individual chromosomes' genetic contributions to the trait to drift upwards or downwards, subject only to the constraint that they all sum to the trait optimum. This chromosome-specific drift causes reduced fitness in individuals with unusual chromosomal constitutions, such as the novel sexual genotypes that sex chromosome turnovers always produce. The theory can explain a suite of patterns in the phylogenetic distribution of sex determining systems. Applied to interspecific hybrids, it can also explain two key observations concerning their reduced fitness: Haldane's rule and the large-X effect.

The theory rests on three assumptions, all empirically supported. First, it requires that some quantitative traits—continuously distributed and controlled by many genes throughout the genome—are under stabilizing selection. Most heritable traits are polygenic, and empirical evidence and theoretical expectation point to many of these traits being under stabilizing selection (Boyle et al. 2017, Sanjak et al. 2018, Sella & Barton 2019, Simons et al. 2018). Second, the theory requires that the genes controlling these traits have different—though perhaps correlated—effects in males and females. Many quantitative traits have a shared, but not identical, genetic architecture in males and females, reflecting the degree of sexual dimorphism in these phenotypes (Poissant et al. 2010, Kassam et al. 2016, Sanjak et al. 2018, Zhu et al. 2023). Third, the theory requires that the sex chromosomes do not recombine along at least a portion of their length in the heterogametic sex. Recombination shutdown between the X and Y (or Z and W) chromosomes is a common property of heterogametic systems, including young ones in which the sex chromosomes have not substantially diverged (Bachtrog et al. 2014, Wright et al. 2016, Jeffries et al. 2018).

Under stabilizing selection, the additive genetic value of a quantitative trait rapidly evolves to the trait optimum, where it is then constrained by selection to remain (Lande 1976). However, while the genome-wide genetic value is constrained to equal the trait optimum, this is not true for subregions of the genome such as individual chromosomes. Instead, their average genetic values can drift upwards or downwards, subject only to the constraint that together their sum must equal the optimum. Thus, for example, chromosome 1's average genetic value for the trait can increase if this is compensated for by a decrease in chromosome 2's average genetic value. The resulting process of constrained drift can be modelled as a system of coupled stochastic differential equations (SI Section S1), revealing that individual chromosomes' genetic values can diverge rapidly even under strong stabilizing selection (Fig. 1a).

The inevitable drift of individual chromosomes' genetic values has important implications for transitions between sex chromosome systems. All such transitions—whether or not they recruit a new linkage group in sex determination, and whether or not they switch the system of heterogamety—generate novel sexual genotypes; that is, male or female genotypes that were not present in the initial sex chromosome system (Fig. 2). These new sexual genotypes disrupt the cross-chromosome balancing act that had maintained quantitative traits at their optimal values under the original sex-determining system. The displacement from trait optima of individuals carrying novel sexual genotypes, and the concomitant reduction in their fitness, creates a barrier to the invasion of the new sex chromosome system (Fig. 2, S1).

This barrier is quantitatively relevant under reasonable parameter regimes (Fig. 2, S2, S3). It hinders sex chromosome turnovers more strongly if the resident sex chromosome system has been maintained for a longer time (Fig. 2); under stronger stabilizing selection (Fig. S2); and under more sex-specific genetic architectures (Fig. S3). Because the barrier relies on the random drift of chromosomes' average genetic values, which is faster in smaller populations (SI Section S1), it will inhibit sex chromosome turnover more strongly in smaller populations, all else equal (Fig. S4, S5). The strength of the barrier also increases with the number of traits under stabilizing selection (Fig. S6), an important feature given the ubiquity of stabilizing selection (Blows & Walsh 2009, Sanjak et al. 2018, Simons et al. 2018, Sella & Barton 2019). Furthermore, though I have assumed an additive genetic basis for traits under selection (Hill et al. 2008, Sella & Barton 2019), non-additive allelic interactions between loci (epistasis) or within loci (dominance) will exacerbate the fitness costs to novel sexual genotypes, and thus strengthen the barrier.

Turnovers in the system of heterogamety that involve new dominant major sex-determining genes produce, in their course, females that carry former Y chromosomes or males that carry former W chromosomes. Such turnovers will be especially disfavored under stabilizing selection since, for example, the Y chromosome from an initial male-heterogametic system was previously carried only by males, allowing its female genetic value for the trait to have drifted unconstrainedly. Females who subsequently come to carry the Y will therefore deviate especially far from the trait optimum. The theory thus

predicts that turnovers involving dominant major sex-determining genes should tend to preserve, rather than change, the system of heterogamety, a prediction that is borne out in phylogenetically rigorous analyses of sex chromosome turnovers in true frogs (Jeffries et al. 2018).

Because any sex chromosome turnover involves the generation of novel sexual genotypes (Bull 1983), stabilizing selection is a global force promoting stability of sex chromosome systems. It can therefore explain the rarity of certain modes of sex chromosome turnover that other theories struggle to explain. For instance, turnovers in the linkage group that determines sex without a change in the system of heterogamety can occur readily under alternative theories but, because these turnovers produce males homozygous for the former X chromosome (or females homozygous for the former Z), they are hindered under stabilizing selection (Fig. 2). Additionally, certain heterologous transitions between male and female heterogamety do not produce YY males or WW females (Bull 1983); the infrequency of these transitions cannot be explained by theories based on large fitness costs to YY or WW individuals but can be explained by the present theory of stabilizing selection (Fig. S7).

The theory can also explain the empirical predominance of transitions from environmental sex determination (ESD) to genetic sex determination (GSD) versus the reverse (Bachtrog et al. 2014, Pennell et al. 2018). Under ESD, all chromosomes are autosomes. The transformation of one pair to sex chromosomes via a new sex-determining mutation (or mutations) does not alter the chromosomal complement of either males or females, and is therefore not disfavored by stabilizing selection. However, the reverse transition from GSD to ESD produces males homozygous for the former X chromosome or females homozygous for the former Z, and is therefore hindered by stabilizing selection.

Thus far, I have described the theory in terms of stabilizing selection around a constant optimal trait value. However, adaptive landscapes are often dynamic (Lande & Arnold 1983, Gibbs & Grant 1987, Stroud et al. 2023). If the optimal trait value shifts, the population experiences directional selection towards the new optimum, which is attained via concerted small changes in allele frequencies at many loci throughout the genome; once the new optimum is reached, stabilizing selection resumes (Lande 1976, Thornton 2019, Hayward & Sella 2022). Thus, the average genetic values of the chromosomes all shift coordinately during the phase of directional selection (Fig. S8), after which they resume the constrained drift process described above. Therefore, the fitness disadvantages suffered by novel sexual genotypes are not, in the long run, impacted by the shift in trait optimum. However, they are attenuated transiently during the period of directional selection (Fig. 3), suggesting that turnovers in sex chromosome systems may be more likely immediately following environmental disturbances or other events that shift the fitness landscape.

Of particular interest is the case where the optimum shifts differently for males and females, inducing sexually antagonistic selection and ultimately sexual dimorphism in the

trait (Fig. 3). Sexually antagonistic optimum shifts provoke disproportionate sex-specific changes in the genetic values of the sex chromosomes relative to the autosomes. Under male heterogamety, the Y exclusively promotes evolution towards the new male optimum, while the X predominantly promotes evolution towards the new female optimum (Muralidhar & Coop 2024) (Fig. S9). The sex chromosomes therefore come to contribute uniquely and disproportionately to the maintenance of male and female trait optima (Fig. 3, Fig. S8), exacerbating the fitness costs suffered by novel sexual genotypes during a sex chromosome transition, as chromosomes that have evolved to promote one sex's trait optimum versus the other's find themselves in the other sex. Moreover, since this effect is a result of directional selection on, rather than constrained drift of, chromosomes' genetic values, it is established on a much faster timescale. Sex chromosome stability has traditionally been studied as a cause of sexual dimorphism (Rice 1984, Mank 2009). Intriguingly, the effect just described suggests a reverse causality, with the outsized role of the sex chromosomes in the evolution of sexual dimorphism stabilizing the sex chromosome system. Teasing apart these directions of causality may soon be possible via phylogenetic methods applied to new, large-scale data on sex-determining mechanisms across diverse taxa (Bachtrog et al. 2014, Vicoso 2019, Ma & Veltsos 2021, Stöck et al. 2021).

It is important to note that the theory described here does not preclude sex chromosome turnovers entirely. It does, however, imply that the forces driving them, such as sexually antagonistic (van Doorn & Kirkpatrick 2007, 2010) or sex-differential (Charnov & Bull 1977) selection, must be sufficiently strong to overcome the fitness disadvantages to novel sexual genotypes under stabilizing selection. In this way, chromosome-specific drift acts as a 'ticking clock': once a new sex chromosome system has evolved, the sex chromosomes drift increasingly over time in their average genetic values for traits under stabilizing selection, gradually decreasing the chance that another transition will be possible. The theory thus predicts that species with young sex chromosome systems are more likely to experience another turnover, relative to species with more established sex chromosome systems. This time constraint will be particularly relevant to heterologous transitions in the heterogametic system, in which former autosomes come to act as neo sex-chromosomes, presenting a clean slate for subsequent divergence of the neo-sex chromosomes' genetic values (Fig. 2).

This temporal prediction is supported by phylogenetic evidence in vertebrates, with clades experiencing either frequent transitions or near-complete stasis (Bachtrog et al 2014, Jeffries et al. 2018, Vicoso 2019, El Taher et al. 2021). However, it is important to note that the mechanism proposed here will act in conjunction with alternative mechanisms promoting the stability of sex chromosome systems over time, such as the accumulation of sexually antagonistic mutations on the sex-specific chromosome (Bull 1983, Rice 1987, Charlesworth et al. 2005) or the evolution of regulatory divergence between the sex chromosomes (Lenormand & Roze 2022).

Under the theory presented here, when the (non-recombining portion of the) sex chromosomes contribute a greater fraction of the genetic variance of traits under stabilizing selection, the selective costs associated with novel sexual genotypes accumulate more rapidly (SI Section S1, Fig. S10). The theory therefore predicts that clades in which the sex chromosomes make up a larger fraction of the genome will experience fewer turnovers, and that the rate of turnovers will be sensitive to the size of the recombining portion of the sex chromosomes (the pseudo-autosomal region) and to other mechanisms that permit XY (or ZW) recombination. One such mechanism is environmentally-induced sex reversal, common in amphibians (Perrin 2009, Flament 2016, Ruiz-García et al. 2021). Recombination patterns in sex-reversed individuals usually accord with their phenotypic, not genotypic, sex (Rodrigues et al. 2018, Perrin 2021), allowing the X and Y (or Z and W) to recombine, slowing the divergence of their genetic values and thus the accumulation of barriers to sex chromosome turnover (Fig. S11).

Although I have focused on its consequences for sex chromosome turnover, chromosome-specific drift under stabilizing selection is important in other evolutionary settings as well. For example, admixture between distinct species in which chromosomes' genetic values have independently coevolved under stabilizing selection generates hybrid individuals with mosaic chromosomal complements. The disruption in these hybrids of the within-species co-adaptation of chromosomes' values causes them to have unfit phenotypes, leading ultimately to selection against introgression (Veller & Simons 2024, Ragsdale 2024).

Stabilizing selection can furthermore explain two key phenomena associated with hybridization: Haldane's Rule and the large-X effect. Haldane's Rule is the observation that, among first-generation (F1) hybrids, when one sex suffers disproportionately large fitness costs, it is usually the heterogametic sex (Schilthuizen et al. 2011, Cutter 2024). The large-X effect refers to the often disproportionate effect of the X (or Z) chromosome in the reduced fitness of hybrids (Presgraves 2008).

To see that chromosome-specific drift under stabilizing selection can account for these phenomena, consider an XY system. Female F1s inherit one X–autosome set from each species; each set was internally co-adapted within its source species, and so female F1s do not suffer reduced fitness under stabilizing selection. However, male F1s inherit an X from one species and a Y from the other—these are not co-adapted (though the X and Y were co-adapted within each source species). Therefore, male F1s will be unfit under stabilizing selection. This presents a novel explanation, compatible with predictions from prior theory and supported by empirical data, for Haldane's Rule (Turelli & Orr 1995, Presgraves 2008, Veller et al. 2023, Xiong et al. 2023, Lenormand & Roze 2024).

The theory can explain the large-X effect too, because of sex chromosomes' unique contributions to the evolution of sexual dimorphism in quantitative traits (Lande 1980, Muralidhar & Coop 2024). With their outsized role in maintaining sexually dimorphic optima, substitutions of these chromosomes via hybridization will generate particularly strong fitness costs owing to selection on the sexually dimorphic trait. The theory thus

predicts that the large-X effect will be more extreme in clades with greater sexual dimorphism and between species with different degrees of sexual dimorphism. With the growing availability of genomic data from hybrid zones, this prediction will soon be testable across a phylogenetically diverse range of taxa (Edelman et al. 2019, Suvorov et al. 2022, Langdon et al. 2022, Vilgalys et al. 2022).

The theory proposed here is similar in kind to theories of "developmental systems drift" (True & Haag 2001, Schiffman & Ralph 2022) where, for example, the individual components of a developmental system (Wang & Sommer 2011, Verster et al. 2014) or regulatory network (Metzger & Wittkop 2019) can undergo evolutionary change while together maintaining a constant phenotypic effect. An advantage of the present theory is that it is cast in concrete population genetic terms—genetic variances, population sizes, selection strengths—so that its consequences, such as for the rate of accumulation of fitness disadvantages to novel sexual genotypes or interspecific hybrids, can be analyzed using the machinery of modern population genetic theory.

Acknowledgements

I thank C. Veller for research assistance and comments on the manuscript. I am grateful to I. Qureshi for comments on the manuscript and G.Coop, J.Berg, M. Steinrücken, L. Delph, M. Hahn, and A. Dahl for helpful discussions. I am also grateful to B.Haller and M. Jarsulic for advice on simulations. The simulations in this paper were run on the Randi computing cluster, supported by the Center for Research Informatics in the Biological Sciences Division at the University of Chicago, and Midway 3 computing cluster, supported by the Research Computing Center at the University of Chicago.

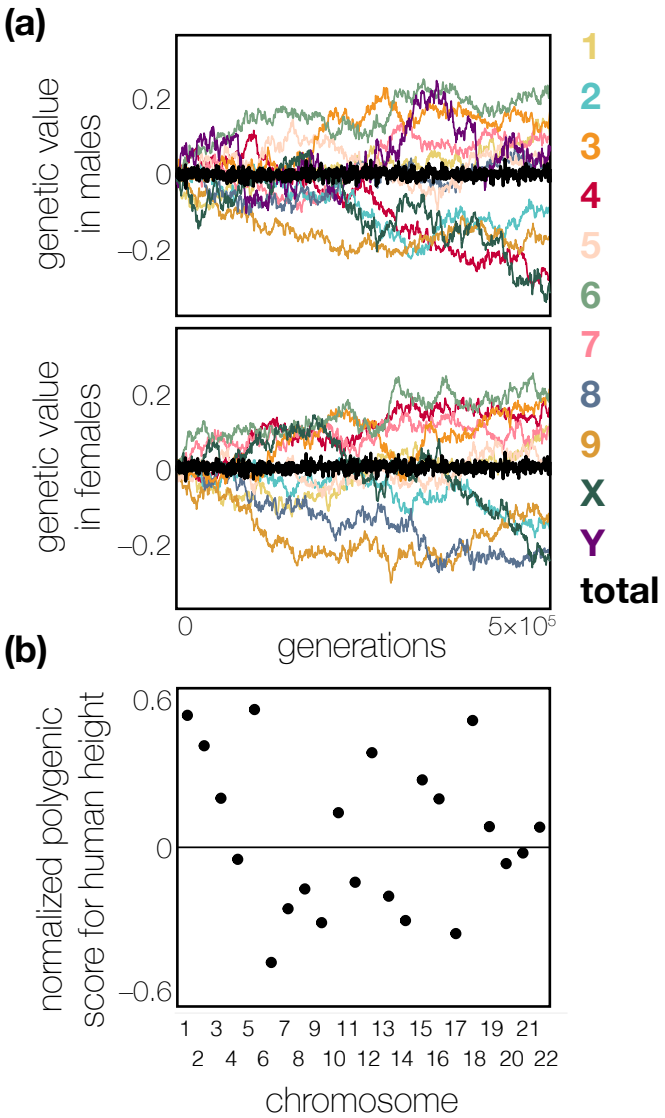

Fig. 1 | Chromosome-specific drift of genetic values for a trait under stabilizing selection. (a) Male and female genetic values of 10 chromosomes in a simulation of a polygenic trait under stabilizing selection around an optimum of 0. The genome-wide mean value remains close to 0 in both sexes (black trajectories), but the values of individual chromosomes vary increasingly over time (colored trajectories). Simulation details in Methods. **(b)** Variance across human autosomes in their average polygenic scores (PGSs) for height, a quantitative trait under stabilizing selection (Sanjak et al. 2018). Chromosome-specific PGSs were calculated using allele frequencies and GWAS effect sizes reported in Yengo et al. 2022 and normalized by the average genome-wide value. Because the PGSs depend only on currently segregating genetic polymorphisms, they likely underestimate the true variation across chromosomes in their average genetic values for height.

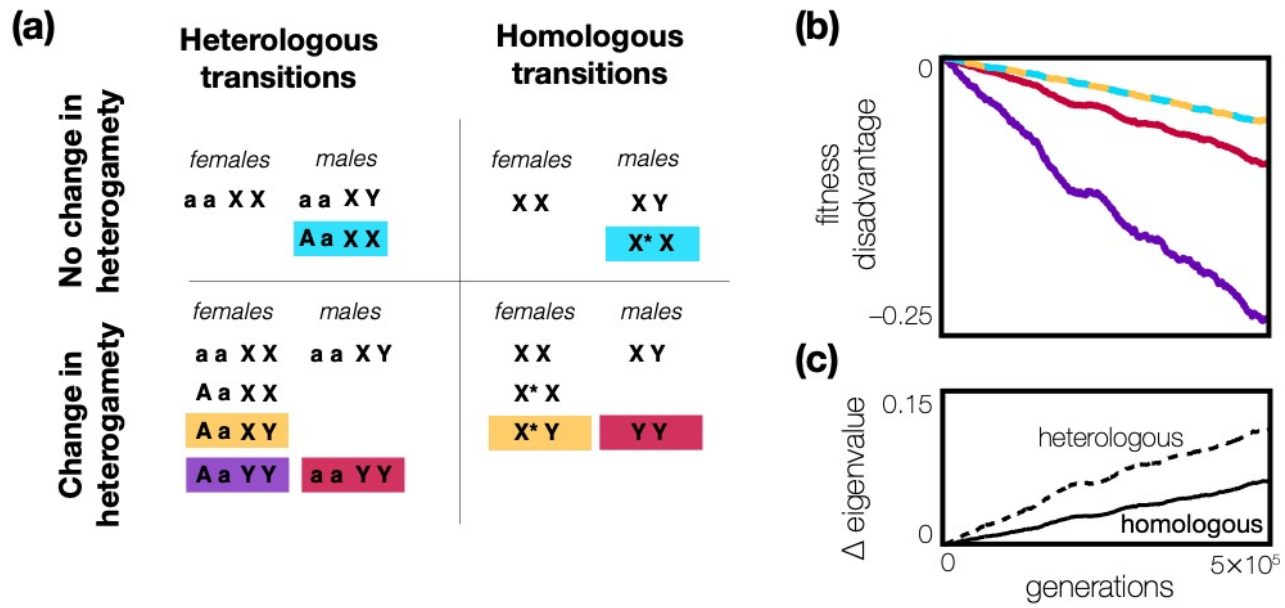

Fig. 2 | Chromosome-specific drift generates increasing barriers to sex chromosome turnover. (a) Sex chromosome turnovers always involve the creation of new sexual genotypes, whether they involve a new linkage group in sex determination (heterologous transitions; left) or not (homologous transitions; right), whether they change the heterogametic system (bottom) or not (top), and whether the new sex-determining mutations involved are dominant (here) or recessive (Fig. S7). **(b)** Chromosome-specific drift for the value of a trait under stabilizing selection generates fitness costs to these novel sexual genotypes, which grow with the age of the original sex chromosome regime. **(c)** The fitness disadvantages to novel sexual genotypes present a barrier to sex chromosome turnover. The strength of the barrier can be measured as the reduction of the eigenvalue of the dynamical system that corresponds to the eigenvector pointing in the direction of the turnover (details in SI Section S2). The reduction of this eigenvalue over time is shown here for homologous and heterologous turnovers of the heterogametic system. In the simulations displayed in **b** and **c**, there is a single trait under selection, and the strength of selection has been chosen to match that inferred for human height (Sanjak et al 2018).

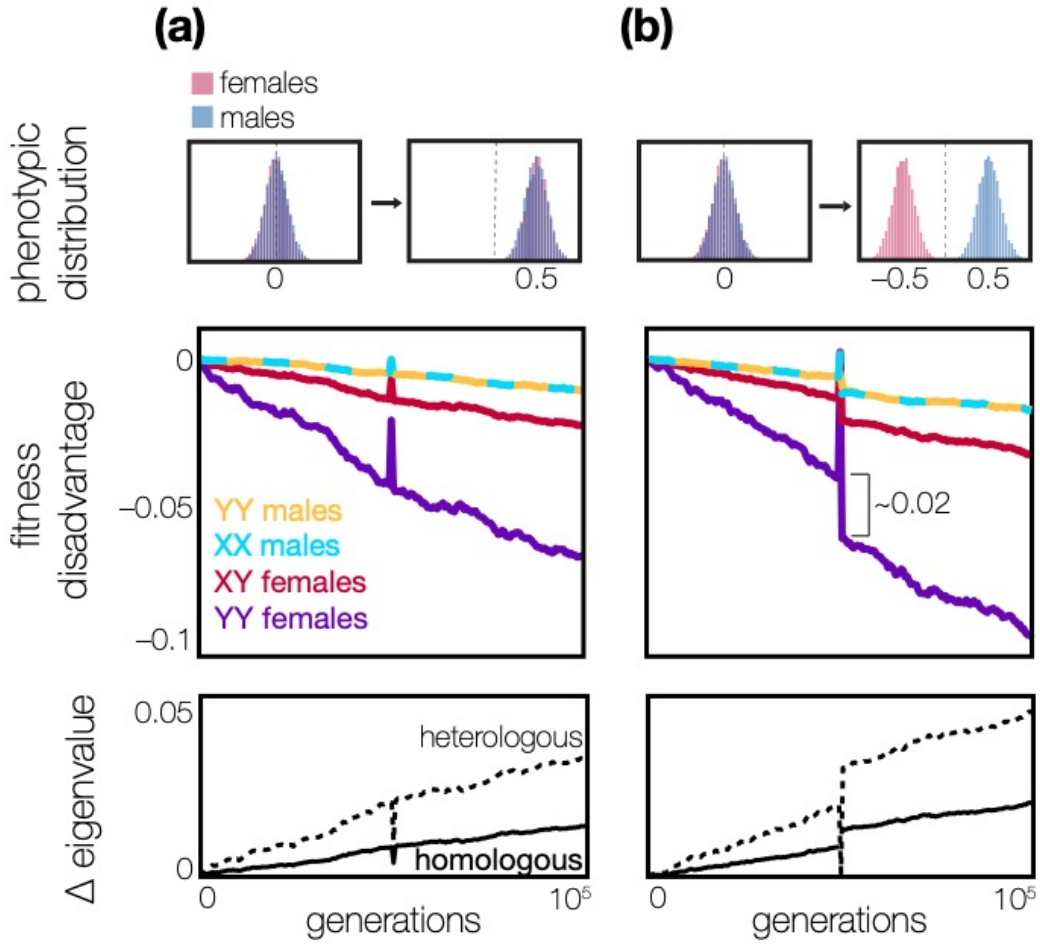

Fig. 3 | Sexually antagonistic shifts in fitness optima strengthen barriers to sex chromosome turnover, while sexually concordant shifts do not. **(a)** When a trait's optimum shifts in the same direction for males and females, the genetic values of all chromosomes shift in concert in the same direction (Fig. S8), and so there is no lasting effect of the shift on the fitness of novel sexual genotypes and therefore the strength of the barrier to sex chromosome turnover, relative to the case of no optimum shift. **(b)** If the trait optimum shifts in different directions for males and females, the X and Y chromosomes uniquely and disproportionately contribute to evolution towards these new optima (Muralidhar & Coop 2024) (Fig. S8, S9). This causes a lasting reduction in the fitness of novel sexual genotypes, which involve imbalances of the original X and/or Y, and a concomitant strengthening of the barrier to sex chromosome turnover. In both sexually concordant and antagonistic optimum shifts, however, the fitness costs to novel sexual genotypes are transiently lowered in the generations immediately following the optimum shift, rendering these brief periods especially conducive to sex chromosome turnover.

Methods

Simulations

Main model. The population is composed of N = 10,000 diploid individuals (5,000 males and 5,000 females) and evolves according to a Wright-Fisher process with random mating. Stabilizing selection is implemented via a Gaussian fitness function with a standard deviation normalized to 1. Unless otherwise stated, males and females have the same optimal phenotype, arbitrarily coded as 0. Under the simulation parameters described below, the strength of stabilizing selection, measured as the ratio between the standard deviation of the fitness function and the standard deviation of the phenotypic distribution, is approximately 5. This strength is similar to empirical estimates of the strength of stabilizing selection on quantitative traits in humans (Sanjak et al 2018, Yair & Coop 2022) and other taxa (de Villemereuil et al. 2022).

An individual's genome is composed of L = 1,000 loci, approximating a quantitative phenotype controlled by 1000 'causal' genes. These 1,000 loci are evenly distributed across 10 chromosomes (9 autosomes and an X and Y chromosome pair). Recombination occurs freely between chromosomes (r = 0.5). The recombination rate between adjacent loci on the autosomes in both sexes and the X chromosome in females is 0.01, so that each chromosome experiences one crossover per gamete on average. There is no crossover interference. Unless otherwise noted, the X and Y chromosomes do not recombine.

The genetic basis of the quantitative trait is additive, such that an individual's trait value is the sum of the phenotypic effects of all of the alleles that they carry. Allelic variation arises in the simulations via mutations, which occur at rate $u = 10^{-5}$ per locus per generation, resulting in a genome-wide mutation rate of $U = Lu$ = 0.01 per generation. The male and female phenotypic effects of new mutations are drawn from a bivariate normal distribution with mean 0, standard deviation 0.05, and correlation ρ = 0.9, so that the phenotypic effects of alleles in males and females are highly, but not perfectly, correlated.

Simulations were initialized with a burn-in period of 10N generations. All calculations were performed relative to the state of the population at the end of this burn-in period. For all fitness calculations, the fitness disadvantage of individuals with novel sexual genotypes is calculated relative to the fitness of individuals with the original sexual genotypes (XY males and XX females).

Simulations were carried out in SLiM 4.1 (Haller & Messer 2023). Unless otherwise noted, results shown in the Main Text are averaged across 500 independent replicates, while results shown in the supplementary figures are averaged across 250 independent replicates. Simulation code is available at: https://github.com/Pavitra451/polygenic_barriers_to_sex_chromosome_turnover/.

Optimum shift. In simulations which involve a shift in fitness optimum, an instantaneous shift in the fitness optima of males and females occurs 5*N* generations after the conclusion of the burn-in period. This shift was either concordant between the sexes, with the male and female fitness optima changing to the same value of 0.5, or sexually antagonistic, with the male optimum increasing to 0.5 and the female optimum decreasing by the same amount to –0.5.

Environmental sex reversal. In simulations examining the effects of environmental sex reversal, 0.5% of genetic males and 0.5% of genetic females undergo sex reversal per generation, such that their genotypic sex does not correspond to their phenotypic sex as an adult. These individuals were selected randomly and suffered no fitness disadvantage independent of their value of the trait under stabilizing selection. In accord with common observation (Rodrigues et al. 2018, Perrin 2021), recombination patterns in sex-reversed individuals were assumed to follow their phenotypic, not genotypic, sex. Thus, for example, the X and Y chromosomes could recombine in sex-reversed XY females.

Multiple traits. To model a scenario where multiple traits under selection are affected by closely linked genes on each chromosome, I implemented two distinct mutational processes across all 1000 loci. Both mutational processes followed the parameters described above, but the first type affected only phenotype 1, while the second type affected only phenotype 2. Both phenotypes experienced the same intensity of stabilizing selection as in the main model. Each individual's overall fitness was the product of their fitness values calculated independently for each trait.

Analysis of human height

The chromosome-specific additive genetic values displayed in Fig. 1b were calculated using summary statistics from the meta-analysis of human height GWASs by Yengo et al. 2022, downloaded from the Giant Consortium website (https://portals.broadinstitute.org/collaboration/giant/index.php/GIANT_consortium_data_files; data file labelled 'Yengo.2022.height.GWAS.ALL'). The X chromosome was excluded from these analyses. The estimated effect of each variant was averaged across males and females.

The polygenic score (PGS) of each autosome was calculated as the sum of the effects of the variants contained on the autosome, weighted by their frequencies. The PGS for each autosome was then normalized by the genome-wide value, to identify relatively height-increasing and height-decreasing chromosomes. Note that, because this analysis is based on GWAS effect sizes, it takes into account only the effects of variants that are segregating in the sampled populations; it does not include fixed variants, which also contribute to differences across chromosomes in their mean genetic values, or variants not segregating in the sampled populations but segregating in other populations. The differences between chromosomes displayed in Fig. 1b is therefore likely an underestimate of the true differences across human autosomes in their genetic values for height.

References

Bachtrog, D., Mank, J. E., Peichel, C. L., Kirkpatrick, M., Otto, S. P., Ashman, T. L., ... & Tree of Sex Consortium. (2014). Sex determination: why so many ways of doing it? *PLoS Biology*, *12*(7), e1001899.

Boyle, E. A., Li, Y. I., & Pritchard, J. K. (2017). An expanded view of complex traits: from polygenic to omnigenic. *Cell*, *169*(7), 1177-1186.

Blows, M., & Walsh, B. (2009). Spherical Cows Grazing in Flatland: Constraints to Selection and Adaptation. In: van der Werf, J., Graser, HU., Frankham, R., Gondro, C. (eds) Adaptation and Fitness in Animal Populations (pp. 83-101). Springer, Dordrecht.

Bull, J. J. (1983). *Evolution of Sex Determining Mechanisms* (Benjamin Cummings, Menlo Park).

Charnov, E. L., & Bull, J. (1977). When is sex environmentally determined? *Nature*, *266*(5605), 828-830.

Charlesworth, D., Charlesworth, B., & Marais, G. (2005). Steps in the evolution of heteromorphic sex chromosomes. *Heredity*, *95*(2), 118-128.

Cutter, A. D. (2024). Beyond Haldane's rule: Sex-biased hybrid dysfunction for all modes of sex determination. *eLife*, *13*, e96652.

de Villemereuil, P., Charmantier, A., Arlt, D., Bize, P., Brekke, P., Brouwer, L., ... & Chevin, L. M. (2020). Fluctuating optimum and temporally variable selection on breeding date in birds and mammals. *Proceedings of the National Academy of Sciences*, *117*(50), 31969-31978.

Edelman, N. B., Frandsen, P. B., Miyagi, M., Clavijo, B., Davey, J., Dikow, R. B., ... & Mallet, J. (2019). Genomic architecture and introgression shape a butterfly radiation. *Science*, *366*(6465), 594-599.

El Taher, A., Ronco, F., Matschiner, M., Salzburger, W., & Böhne, A. (2021). Dynamics of sex chromosome evolution in a rapid radiation of cichlid fishes. *Science Advances*, *7*(36), eabe8215.

Flament, S. (2016). Sex reversal in amphibians. *Sexual Development*, *10*(5-6), 267-278.

Gibbs, H. L., & Grant, P. R. (1987). Oscillating selection on Darwin's finches. *Nature*, *327*(6122), 511-513.

Haller, B. C., & Messer, P. W. (2023). SLiM 4: multispecies eco-evolutionary modeling. *The American Naturalist*, *201*(5), E127-E139.

Hayward, L. K., & Sella, G. (2022). Polygenic adaptation after a sudden change in environment. *Elife*, *11*, e66697.

Hill, W. G., Goddard, M. E., & Visscher, P. M. (2008). Data and theory point to mainly additive genetic variance for complex traits. *PLoS genetics*, *4*(2), e1000008.

Jeffries, D. L., Lavanchy, G., Sermier, R., Sredl, M. J., Miura, I., Borzée, A., ... & Perrin, N. (2018). A rapid rate of sex-chromosome turnover and non-random transitions in true frogs. *Nature Communications*, *9*(1), 4088.

Kassam, I., Lloyd-Jones, L., Holloway, A., Small, K. S., Zeng, B., Bakshi, A., ... & McRae, A. F. (2016). Autosomal genetic control of human gene expression does not differ across the sexes. *Genome Biology*, *17*, 1-10.

Lande, R. (1976). Natural selection and random genetic drift in phenotypic evolution. *Evolution*, 314-334.

Lande, R. (1980). Sexual dimorphism, sexual selection, and adaptation in polygenic characters. *Evolution*, 292-305.

Lande, R., & Arnold, S. J. (1983). The measurement of selection on correlated characters. *Evolution*, 1210-1226.

Langdon, Q. K., Powell, D. L., Kim, B., Banerjee, S. M., Payne, C., Dodge, T. O., ... & Schumer, M. (2022). Predictability and parallelism in the contemporary evolution of hybrid genomes. *PLoS Genetics*, *18*(1), e1009914.

Lenormand, T., & Roze, D. (2022). Y recombination arrest and degeneration in the absence of sexual dimorphism. *Science*, *375*(6581), 663-666.

Lenormand, T., & Roze, D. (2024). A single theory for the evolution of sex chromosomes and the two rules of speciation. *bioRxiv*. doi: https://doi.org/10.1101/2024.03.18.585601

Ma, W. J., & Veltsos, P. (2021). The diversity and evolution of sex chromosomes in frogs. *Genes*, *12*(4), 483.

Mank, J. E. (2009). Sex chromosomes and the evolution of sexual dimorphism: lessons from the genome. *The American Naturalist*, *173*(2), 141-150.

Metzger, B. P., & Wittkopp, P. J. (2019). Compensatory *trans*-regulatory alleles minimizing variation in *TDH3* expression are common within *Saccharomyces cerevisiae*. *Evolution Letters*, *3*(5), 448-461.

Muralidhar, P., & Veller, C. (2018). Sexual antagonism and the instability of environmental sex determination. *Nature Ecology & Evolution*, *2*(2), 343-351.

Muralidhar, P., & Coop, G. (2024). Polygenic response of sex chromosomes to sexual antagonism. *Evolution*, *78*(3), 539-554.

Pennell, M. W., Mank, J. E., & Peichel, C. L. (2018). Transitions in sex determination and sex chromosomes across vertebrate species. *Molecular Ecology*, *27*(19), 3950-3963.

Perrin, N. (2009). Sex reversal: a fountain of youth for sex chromosomes? *Evolution*, *63*(12), 3043-3049.

Perrin, N. (2021). Sex-chromosome evolution in frogs: what role for sex-antagonistic genes? *Philosophical Transactions of the Royal Society B*, *376*(1832), 20200094.

Poissant, J., Wilson, A. J., & Coltman, D. W. (2010). Sex-specific genetic variance and the evolution of sexual dimorphism: a systematic review of cross-sex genetic correlations. *Evolution*, *64*(1), 97-107.

Presgraves, D. C. (2008). Sex chromosomes and speciation in *Drosophila*. *Trends in Genetics*, *24*(7), 336-343.

Ragsdale, A. P. (2024). Archaic introgression and the distribution of shared variation under stabilizing selection. *bioRxiv*. doi: https://doi.org/10.1101/2024.08.20.608876

Rice, W. R. (1984). Sex chromosomes and the evolution of sexual dimorphism. *Evolution*, 735-742.

Rice, W. R. (1987). The accumulation of sexually antagonistic genes as a selective agent promoting the evolution of reduced recombination between primitive sex chromosomes. *Evolution*, *41*(4), 911-914.

Rodrigues, N., Studer, T., Dufresnes, C., & Perrin, N. (2018). Sex-chromosome recombination in common frogs brings water to the fountain-of-youth. *Molecular biology and evolution*, *35*(4), 942-948.

Ruiz-García, A., Roco, Á. S., & Bullejos, M. (2021). Sex differentiation in amphibians: effect of temperature and its influence on sex reversal. *Sexual Development*, *15*(1-3), 157-167.

Sanjak, J. S., Sidorenko, J., Robinson, M. R., Thornton, K. R., & Visscher, P. M. (2018). Evidence of directional and stabilizing selection in contemporary humans. *Proceedings of the National Academy of Sciences*, *115*(1), 151-156.

Schiffman, J. S., & Ralph, P. L. (2022). System drift and speciation. *Evolution*, *76*(2), 236-251.

Schilthuizen, M., Giesbers, M. C. W. G., & Beukeboom, L. W. (2011). Haldane's rule in the 21st century. *Heredity*, *107*(2), 95-102.

Sella, G., & Barton, N. H. (2019). Thinking about the evolution of complex traits in the era of genome-wide association studies. *Annual Review of Genomics and Human Genetics*, *20*(1), 461-493.

Simons, Y. B., Bullaughey, K., Hudson, R. R., & Sella, G. (2018). A population genetic interpretation of GWAS findings for human quantitative traits. *PLoS Biology*, *16*(3), e2002985.

Stöck, M., Kratochvíl, L., Kuhl, H., Rovatsos, M., Evans, B. J., Suh, A., ... & Guiguen, Y. (2021). A brief review of vertebrate sex evolution with a pledge for integrative research: towards 'sexomics'. *Philosophical Transactions of the Royal Society B*, *376*(1832), 20200426.

Stroud, J. T., Moore, M. P., Langerhans, R. B., & Losos, J. B. (2023). Fluctuating selection maintains distinct species phenotypes in an ecological community in the wild. *Proceedings of the National Academy of Sciences*, *120*(42), e2222071120.

Suvorov, A., Kim, B. Y., Wang, J., Armstrong, E. E., Peede, D., D'agostino, E. R., ... & Comeault, A. A. (2022). Widespread introgression across a phylogeny of 155 *Drosophila* genomes. *Current Biology*, *32*(1), 111-123.

Thornton, K. R. (2019). Polygenic adaptation to an environmental shift: temporal dynamics of variation under Gaussian stabilizing selection and additive effects on a single trait. *Genetics*, *213*(4), 1513-1530.

True, J. R., & Haag, E. S. (2001). Developmental system drift and flexibility in evolutionary trajectories. *Evolution & Development*, *3*(2), 109-119.

Turelli, M., & Orr, H. A. (1995). The dominance theory of Haldane's rule. *Genetics*, *140*(1), 389-402.

van Doorn, G. S., & Kirkpatrick, M. (2007). Turnover of sex chromosomes induced by sexual conflict. *Nature*, *449*(7164), 909-912.

van Doorn, G. S., & Kirkpatrick, M. (2010). Transitions between male and female heterogamety caused by sex-antagonistic selection. *Genetics*, *186*(2), 629-645.

Veller, C., Edelman, N. B., Muralidhar, P., & Nowak, M. A. (2023). Recombination and selection against introgressed DNA. *Evolution*, *77*(4), 1131-1144.

Veller, C., & Simons, Y. (2024). Stabilizing selection generates selection against introgressed DNA. *bioRxiv*. doi: https://doi.org/10.1101/2024.08.20.608860

Verster, A. J., Ramani, A. K., McKay, S. J., & Fraser, A. G. (2014). Comparative RNAi screens in *C. elegans* and *C. briggsae* reveal the impact of developmental system drift on gene function. *PLoS Genetics*, *10*(2), e1004077.

Vicoso, B. (2019). Molecular and evolutionary dynamics of animal sex-chromosome turnover. *Nature Ecology & Evolution*, *3*(12), 1632-1641.

Vilgalys, T. P., Fogel, A. S., Anderson, J. A., Mututua, R. S., Warutere, J. K., Siodi, I. L. I., ... & Tung, J. (2022). Selection against admixture and gene regulatory divergence in a long-term primate field study. *Science*, *377*(6606), 635-641.

Wang, X., & Sommer, R. J. (2011). Antagonism of LIN-17/Frizzled and LIN-18/Ryk in nematode vulva induction reveals evolutionary alterations in core developmental pathways. *PLoS Biology*, *9*(7), e1001110.

Wright, A. E., Dean, R., Zimmer, F., & Mank, J. E. (2016). How to make a sex chromosome. *Nature Communications*, *7*(1), 12087.

Wright, A. E., Darolti, I., Bloch, N. I., Oostra, V., Sandkam, B., Buechel, S. D., Kolm, N., Breden, F., Vicoso, B. & Mank, J. E. (2017). Convergent recombination suppression suggests role of sexual selection in guppy sex chromosome formation. *Nature Communications*, *8*(1), 14251.

Xiong, T., Tarikere, S., Rosser, N., Li, X., Yago, M., & Mallet, J. (2023). A polygenic explanation for Haldane's rule in butterflies. *Proceedings of the National Academy of Sciences*, *120*(44), e2300959120.

Yair, S., & Coop, G. (2022). Population differentiation of polygenic score predictions under stabilizing selection. *Philosophical Transactions of the Royal Society B*, *377*(1852), 20200416.

Yengo, L., Vedantam, S., Marouli, E., Sidorenko, J., Bartell, E., Sakaue, S., ... & Lee, J. Y. (2022). A saturated map of common genetic variants associated with human height. *Nature*, *610*(7933), 704-712.

Zhu, C., Ming, M. J., Cole, J. M., Edge, M. D., Kirkpatrick, M., & Harpak, A. (2023). Amplification is the primary mode of gene-by-sex interaction in complex human traits. *Cell Genomics*, *3*(5).

Polygenic barriers to sex chromosome turnover
Supplementary Information

Pavitra Muralidhar

S1 Chromosome-specific drift under stabilizing selection

In a diploid, random-mating population of size N, a trait is under Gaussian stabilizing selection of strength V_S around an optimal value of zero. The genetic and phenotypic variance of the trait are V_G and V_P.

Let the mean genetic value of a focal chromosome at time t be $x(t)$, and the mean genetic value of the rest of the genome be $y(t)$, so that the overall mean genetic value is $z(t) = x(t) + y(t)$. If the focal chromosome accounts for a fraction l of the total genetic variance V_G, with the rest of the genome accounting for the remaining fraction $1 - l$, then x and y evolve according to the coupled stochastic differential equations (Veller, Muralidhar, in prep.):

$$\dot{x}(t) = -\frac{lV_G}{V_S + V_P}[x(t) + y(t)] + \sqrt{\frac{lV_G}{N}}\,\xi_1(t), \tag{S.1}$$

$$\dot{y}(t) = -\frac{(1-l)V_G}{V_S + V_P}[x(t) + y(t)] + \sqrt{\frac{(1-l)V_G}{N}}\,\xi_2(t), \tag{S.2}$$

where $\xi_1(t)$ and $\xi_2(t)$ are independent Gaussian white noises with zero mean and unit variance.

Notice that, from Eqs. (S.1) and (S.2),

$$\begin{aligned}\dot{z}(t) = \dot{x}(t) + \dot{y}(t) &= -\frac{V_G}{V_S + V_P}z(t) + \sqrt{\frac{lV_G}{N}}\,\xi_1(t) + \sqrt{\frac{(1-l)V_G}{N}}\,\xi_2(t) \\ &= -\frac{V_G}{V_S + V_P}z(t) + \sqrt{\frac{V_G}{N}}\,\xi_3(t),\end{aligned} \tag{S.3}$$

where $\xi_3(t)$ is a Gaussian white noise with zero mean and unit variance. Eq. (S.3) confirms that, under stabilizing selection, the overall mean genetic value evolves according to an Ornstein–Uhlenbeck process (e.g., Lande 1976).

We now write $u(t) = \frac{x(t)}{l}$ and $v(t) = \frac{y(t)}{1-l}$. Then

$$\dot{u}(t) = \frac{\dot{x}(t)}{l} = -\frac{V_G}{V_S + V_P}[x(t) + y(t)] + \sqrt{\frac{V_G}{lN}}\,\xi_1(t), \tag{S.4}$$

$$\dot{v}(t) = \frac{\dot{y}(t)}{1-l} = -\frac{V_G}{V_S + V_P}[x(t) + y(t)] + \sqrt{\frac{V_G}{(1-l)N}}\,\xi_2(t). \tag{S.5}$$

Define $w(t) = u(t) - v(t)$. Taking the difference of Eqs. (S.4) and (S.5),

$$\dot{w}(t) = \dot{u}(t) - \dot{v}(t) = \sqrt{\frac{V_G}{lN}}\,\xi_1(t) - \sqrt{\frac{V_G}{(1-l)N}}\,\xi_2(t) = \sqrt{\frac{V_G}{l(1-l)N}}\,\xi_4(t),$$

where $\xi_4(t)$ is a Gaussian white noise with zero mean and unit variance. Therefore, $w(t) = \frac{x(t)}{l} - \frac{y(t)}{1-l}$ behaves as a Brownian motion.

Under stabilizing selection, $z(t) = x(t) + y(t) \approx 0$ for all t large enough, and so, eventually, we can approximate $y(t) = -x(t)$. Therefore,

$$w(t) = \frac{x(t)}{l} - \frac{y(t)}{1-l} = \frac{x(t)}{l} + \frac{x(t)}{1-l} = \frac{x(t)}{l(1-l)},$$

and so

$$\dot{x}(t) = l(1-l)\dot{w}(t) = \sqrt{\frac{l(1-l)V_G}{N}}\,\xi_4(t). \tag{S.6}$$

The chromosome-specific mean value $x(t)$ is therefore a Brownian motion. With a starting value $x(0) = 0$, the mean of $x(t)$ is zero and its variance is

$$\mathrm{Var}[x(t)] = \frac{l(1-l)V_G}{N} \cdot t. \tag{S.7}$$

S2 Quantifying the strength of resistance to transitions of heterogamety

S2.1 Heterologous transitions in heterogamety

From an initial system of XX/XY male heterogamety, a mutated autosome A appears that is feminizing and, in this effect, is epistatically dominant to the Y chromosome. If A increases sufficiently in frequency relative to the wild-type a autosome, the system transitions to one in which females have the genotype Aa YY and males have the genotype aa YY, i.e., a system of female heterogamety where A serves as a W chromosome, a serves as a Z chromosome, and the old Y chromosome is now an autosome. The transition between the old aa XX, aa XY system and the new Aa YY, aa YY system involves intermediate states with six sexual genotypes, four female and two male:

	genotype	frequency	relative viability
♀	aa XX	p_1	1
	Aa XX	p_2	1
	Aa XY	p_3	$1-r$
	Aa YY	p_4	$1-s$
♂	aa XY	p_5	1
	aa YY	p_6	$1-t$

Sexual genotypes that were not present in the ancestral system—here, XY females and YY females and males—suffer fitness disadvantages under stabilizing selection, per the argument advanced in the Main Text. These fitness disadvantages are denoted r, s, and t as in the table above.

Given some initial frequencies of the six genotypes, if the fitness disadvantages above are not too large, the frequencies converge rapidly to a 'slow manifold' along which the sex ratio is within a negligible distance of 1/2 (Bull and Charnov 1977; Veller et al. 2017). Label the frequencies of the genotypes $p_1, p_2, \ldots, p_6$ as in the table above, and assume that these frequencies lie on the slow manifold so that,

to leading order, $p_1 + p_2 + p_3 + p_4 = 1/2$ and $p_5 + p_6 = 1/2$. Since the frequencies will stay in the close vicinity of the slow manifold, we need only derive update equations for p_1, p_2, p_3, and p_5.

Define

$$w_{♀} = \tfrac{1}{2} - p_3 r - p_4 s \tag{S.8}$$

$$= \frac{1}{2} - p_3 r - \left(\frac{1}{2} - p_1 - p_2 - p_3\right) s; \tag{S.9}$$

$$w_{♂} = \tfrac{1}{2} - p_6 t \tag{S.10}$$

$$= \frac{1}{2} - \left(\frac{1}{2} - p_5\right) t. \tag{S.11}$$

Then, after viability selection, the fractions of females with genotypes 1, 2, 3, and 4 are $v_1 = p_1/w_{♀}$, $v_2 = p_2/w_{♀}$, $v_3 = p_3(1-r)/w_{♀}$, and $v_4 = p_4(1-s)/w_{♀} = \left(\frac{1}{2} - p_1 - p_2 - p_3\right)(1-s)/w_{♀}$, while the fractions of males with genotypes 5 and 6 are $v_5 = p_5/w_{♂}$ and $v_6 = p_6(1-t)/w_{♂} = \left(\frac{1}{2} - p_5\right)(1-t)/w_{♂}$. Under random mating, the expected frequencies of genotypes 1, 2, 3, and 5 in the next generation are then

$$\begin{aligned}
p_1' &= \frac{1}{2} v_1 v_5 + \frac{1}{4} v_2 v_5 + \frac{1}{8} v_3 v_5 \\
&=: f_1(p_1, p_2, p_3, p_5); \\
p_2' &= \frac{1}{4} v_2 v_5 + \frac{1}{8} v_3 v_5 \\
&=: f_2(p_1, p_2, p_3, p_5); \\
p_3' &= \frac{1}{4} v_2 v_5 + \frac{1}{2} v_2 v_6 + \frac{1}{4} v_3 v_5 + \frac{1}{4} v_3 v_6 + \frac{1}{4} v_4 v_5 \\
&=: f_3(p_1, p_2, p_3, p_5); \\
p_5' &= \frac{1}{2} v_1 v_5 + v_1 v_6 + \frac{1}{4} v_2 v_5 + \frac{1}{2} v_2 v_6 + \frac{1}{4} v_3 v_5 + \frac{1}{4} v_3 v_6 + \frac{1}{4} v_4 v_5 \\
&=: f_5(p_1, p_2, p_3, p_5).
\end{aligned} \tag{S.12}$$

We are interested in the potential for invasion of the initial aa XX, aa XY system, which corresponds to the equilibrium point $p^* = (p_1^*, p_2^*, p_3^*, p_5^*) = (1/2, 0, 0, 1/2)$. The Jacobian matrix of the system, evaluated at this initial point p^*, can be calculated to be

$$J|_{p^*} = \left.\begin{pmatrix} \frac{\partial f_1}{\partial p_1} & \frac{\partial f_1}{\partial p_2} & \frac{\partial f_1}{\partial p_3} & \frac{\partial f_1}{\partial p_4} \\ \frac{\partial f_2}{\partial p_1} & \frac{\partial f_2}{\partial p_2} & \frac{\partial f_2}{\partial p_3} & \frac{\partial f_2}{\partial p_4} \\ \frac{\partial f_3}{\partial p_1} & \frac{\partial f_3}{\partial p_2} & \frac{\partial f_3}{\partial p_3} & \frac{\partial f_3}{\partial p_4} \\ \frac{\partial f_4}{\partial p_1} & \frac{\partial f_4}{\partial p_2} & \frac{\partial f_5}{\partial p_3} & \frac{\partial f_4}{\partial p_4} \end{pmatrix}\right|_{p^*} = \begin{pmatrix} 1-s & \frac{1}{2}-s & \frac{1}{4}-s+\frac{3}{4}r & 1-t \\ 0 & \frac{1}{2} & \frac{1}{4}(1-r) & 0 \\ -\frac{1}{2}(1-s) & \frac{1}{2}s & \frac{1}{2}(s-r) & 0 \\ \frac{1}{2}(1-s) & -\frac{1}{2}s & \frac{1}{2}(r-s) & -(1-t) \end{pmatrix}. \tag{S.13}$$

We are interested in the eigenvalue of this Jacobian matrix that corresponds to the eigenvector $\sim (+0.853; -0.213; -0.426; +0.213)$, which is the eigenvector pointing in the direction of the slow manifold along which invasion of the system would proceed (the vector $(+0.853; -0.213; -0.426; +0.213)$ is the relevant eigenvector in the neutral system, and corresponds to an eigenvalue of 1 in that system).

S2.2 Homologous transitions in heterogamety

From an initial system of XX, XY male heterogamety, a mutated X chromosome X′ appears that is feminizing and, in this effect, is epistatically dominant to the Y chromosome. If X′ increases sufficiently

in frequency relative to the wild-type X, the system transitions to one in which females have the genotype X′Y and males have the genotype YY, i.e., a system of female heterogamety where X′ serves as a W chromosome and Y serves as a Z chromosome. The transition between the old XX, XY system and the new X′Y, YY system involves intermediate states with five sexual genotypes, three female and two male:

	genotype	frequency	relative viability
♀	XX	p_1	1
	X′X	p_2	1
	X′Y	p_3	$1-s$
♂	XY	p_4	1
	YY	p_5	$1-t$

Sexual genotypes that were not present in the ancestral system—here, X′Y females and YY males—suffer fitness disadvantages under stabilizing selection. These fitness disadvantages are denoted s and t respectively in the table above.

Given some initial frequencies of the five genotypes, if the fitness disadvantages above are not too large, then just as in the heterologous system above, the frequencies converge rapidly to a slow manifold along which the sex ratio is within a negligible distance of 1/2 (Bull and Charnov 1977; Veller et al. 2017). Label the frequencies of the genotypes $p_1, p_2, \ldots, p_5$ as in the table above, and assume that these frequencies lie on the slow manifold so that, to leading order, $p_1+p_2+p_3 = 1/2$ and $p_4+p_5 = 1/2$. Since the frequencies will stay in the close vicinity of the slow manifold, we need only derive update equations for p_1, p_2, and p_4.

Define

$$w_{♀} = \tfrac{1}{2} - p_3 s \tag{S.14}$$

$$= \frac{1}{2} - \left(\frac{1}{2} - p_1 - p_2\right) s; \tag{S.15}$$

$$w_{♂} = \tfrac{1}{2} - p_5 t \tag{S.16}$$

$$= \frac{1}{2} - \left(\frac{1}{2} - p_4\right) t. \tag{S.17}$$

Then, after viability selection, the fractions of females with genotypes 1, 2, and 3 are $v_1 = p_1/w_{♀}$ and $v_2 = p_2/w_{♀}$, and $v_3 = p_3(1-s)/w_{♀} = \left(\frac{1}{2} - p_1 - p_2\right)(1-s)/w_{♀}$, while the fractions of males with genotypes 4 and 5 are $v_4 = p_5/w_{♂}$ and $v_5 = p_5(1-t)/w_{♂} = \left(\frac{1}{2} - p_4\right)(1-t)/w_{♂}$. Under random mating, the expected frequencies of genotypes 1, 2, and 4 in the next generation are then

$$\begin{aligned}
p_1' &= \frac{1}{2}v_1v_4 + \frac{1}{4}v_2v_4 \\
&=: f_1(p_1, p_2, p_4); \\
p_2' &= \frac{1}{4}v_2v_4 + \frac{1}{4}v_3v_4 \\
&=: f_2(p_1, p_2, p_3, p_5); \\
p_4' &= \frac{1}{2}v_1v_4 + v_1v_5 + \frac{1}{4}v_2v_4 + \frac{1}{2}v_2v_5 + \frac{1}{4}v_3v_4 \\
&=: f_4(p_1, p_2, p_3, p_5).
\end{aligned} \tag{S.18}$$

We are interested in the potential for invasion of the initial XX, XY system, which corresponds to the equilibrium point $p^* = (p_1^*, p_2^*, p_4^*) = (1/2, 0, 1/2)$. The Jacobian matrix of the system, evaluated at this initial point p^*, can be calculated to be

$$J|_{p^*} = \left.\begin{pmatrix} \frac{\partial f_1}{\partial p_1} & \frac{\partial f_1}{\partial p_2} & \frac{\partial f_1}{\partial p_4} \\ \frac{\partial f_2}{\partial p_1} & \frac{\partial f_2}{\partial p_2} & \frac{\partial f_2}{\partial p_4} \\ \frac{\partial f_4}{\partial p_1} & \frac{\partial f_3}{\partial p_2} & \frac{\partial f_4}{\partial p_4} \end{pmatrix}\right|_{p^*} = \begin{pmatrix} 1-s & \frac{1}{2}-s & 1-t \\ -\frac{1}{2}(1-s) & \frac{1}{2}s & 0 \\ \frac{1}{2}(1-s) & -\frac{1}{2}s & -(1-t) \end{pmatrix}. \tag{S.19}$$

We are interested in the eigenvalue of this Jacobian matrix that corresponds to the eigenvector $\sim (+0.873; -0.436; +0.218)$, which is the eigenvector pointing in the direction of the slow manifold along which invasion of the system would proceed (the vector $(+0.873; -0.436; +0.218)$ is the relevant eigenvector in the neutral system, and corresponds to an eigenvalue of 1 in that system).

References

Bull, J. J. and Charnov, E. L. (1977). Changes in the heterogametic mechanism of sex determination. *Heredity*, 39(1):1–14.

Lande, R. (1976). Natural selection and random genetic drift in phenotypic evolution. *Evolution*, 30(2):314–334.

Veller, C., Muralidhar, P., Constable, G. W., and Nowak, M. A. (2017). Drift-induced selection between male and female heterogamety. *Genetics*, 207(2):711–727.

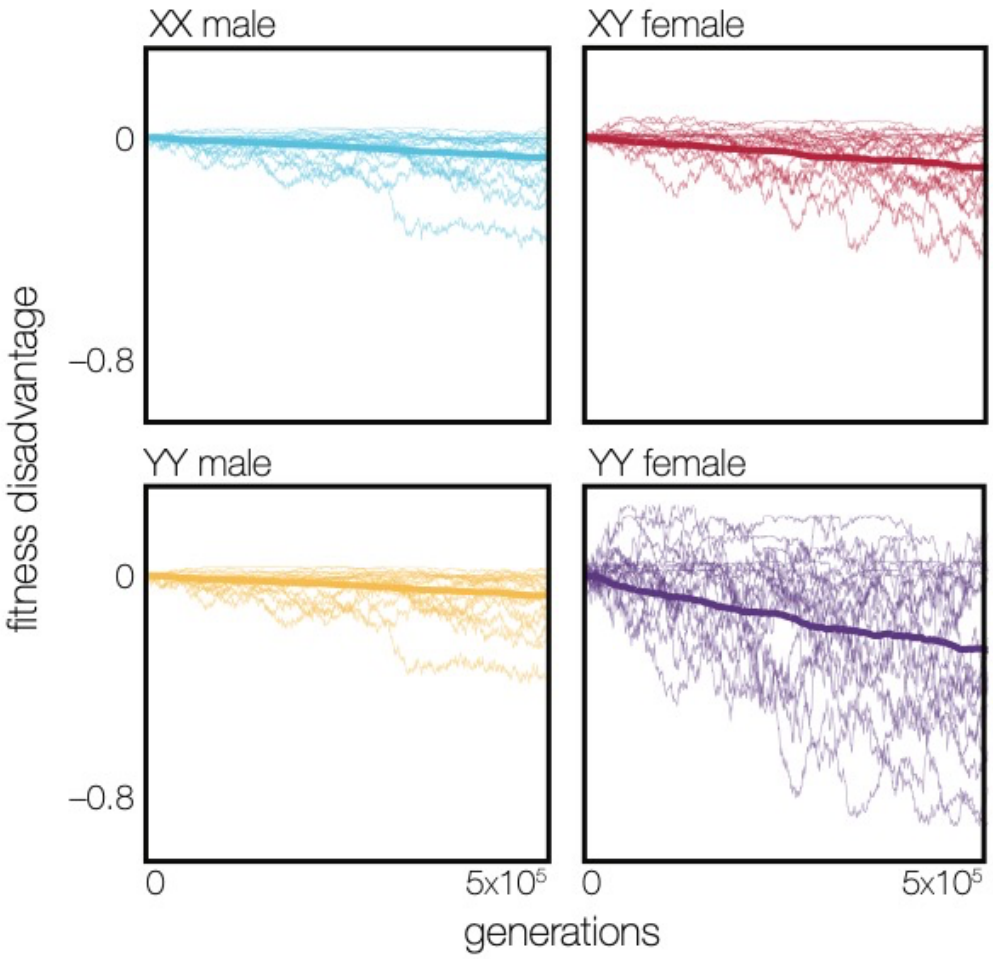

Fig. S1 | The fitness disadvantages associated with novel sexual genotypes reflect the stochasticity of chromosome-specific drift. Each faint line represents the relative fitness reduction to novel sexual genotypes in a single simulation run; 20 independent simulation runs are shown here. Bold lines indicate mean fitness of the sexual genotypes across 500 simulation runs. While the fitness costs to novel sexual genotypes in a particular simulation run are noisy, reflecting the drift-based divergence in each chromosome's genetic value, the overall effect of this chromosome-specific drift is to decrease the fitness of novel sexual genotypes.

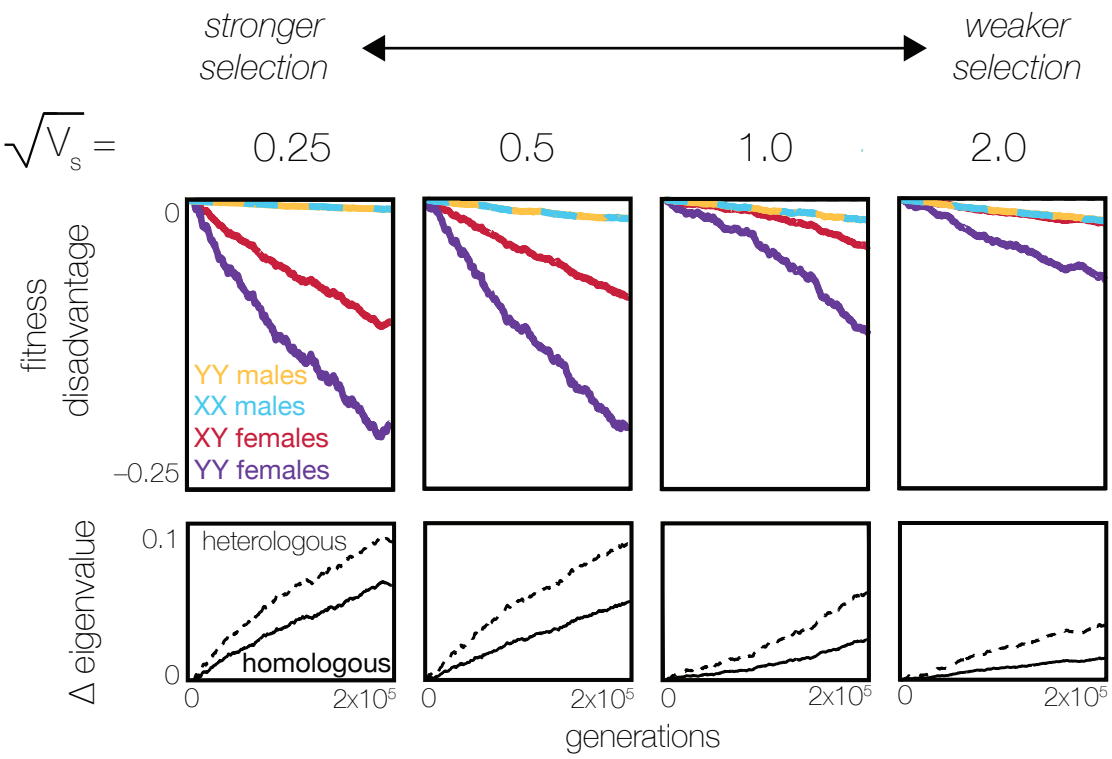

Fig. S2 | Increasing the intensity of stabilizing selection on quantitative traits impedes sex chromosome turnovers. Parameters are the same as in Fig. 2, but here, results are shown for different strengths of selection, parameterized by the width of the Gaussian fitness function $\sqrt{V_s}$ (in Fig. 2, $\sqrt{V_s}$ = 1). Lower values of $\sqrt{V_s}$ correspond to stronger stabilizing selection, which is seen to increase the fitness costs associated with novel sexual genotypes and therefore to decrease the probability of sex chromosome turnover. However, even weak stabilizing selection (e.g., $\sqrt{V_s}$ = 2) can generate significant barriers to sex chromosome turnover on the same time scale.

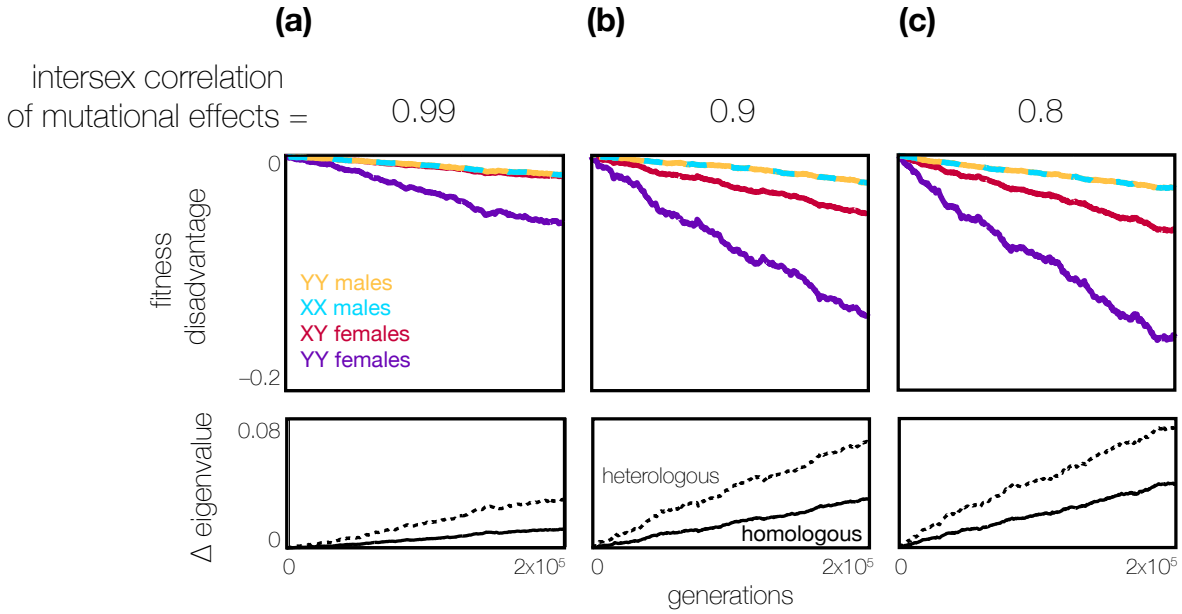

Fig. S3 | Higher sex-specificity in the genetic architecture of quantitative phenotypes enhances barriers to sex chromosome transitions. Parameters are the same as in Fig. 2, but the correlation between the phenotypic effects of new mutations in males and females is (a) 0.99, (b) 0.9, (as Fig. 2), or (c) 0.8, reflecting an increasing degree of sex-specificity in the genetic basis of the trait. A nearly completely shared genetic architecture for the trait in males and females, as in (a), constrains the genetic values on the X and Y chromosomes to resemble each other, reducing the impact of chromosomal re-arrangements and decreasing the selective disadvantages of novel sexual genotypes. In contrast, a more sex-specific genetic architecture, as in (c), allows for greater divergence between the X and Y, and generates stronger barriers to sex chromosome turnover.

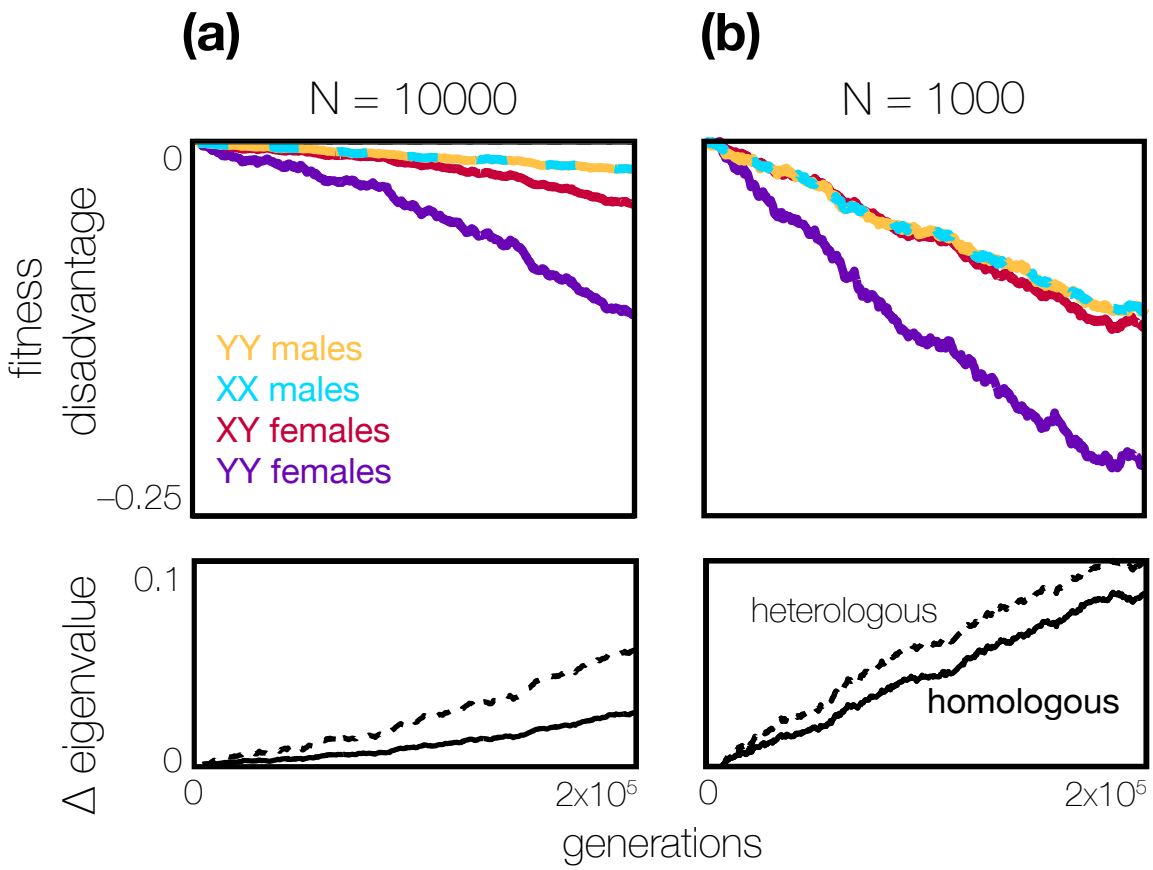

Fig. S4 | Smaller population sizes accelerate chromosome-specific drift, impeding sex chromosome turnovers. Parameters are as in Fig. 2 in (a), but the population size is reduced to N = 1,000 in (b). A smaller population size facilitates chromosome-specific drift, causing the fitness costs to novel sexual genotypes to grow more rapidly.

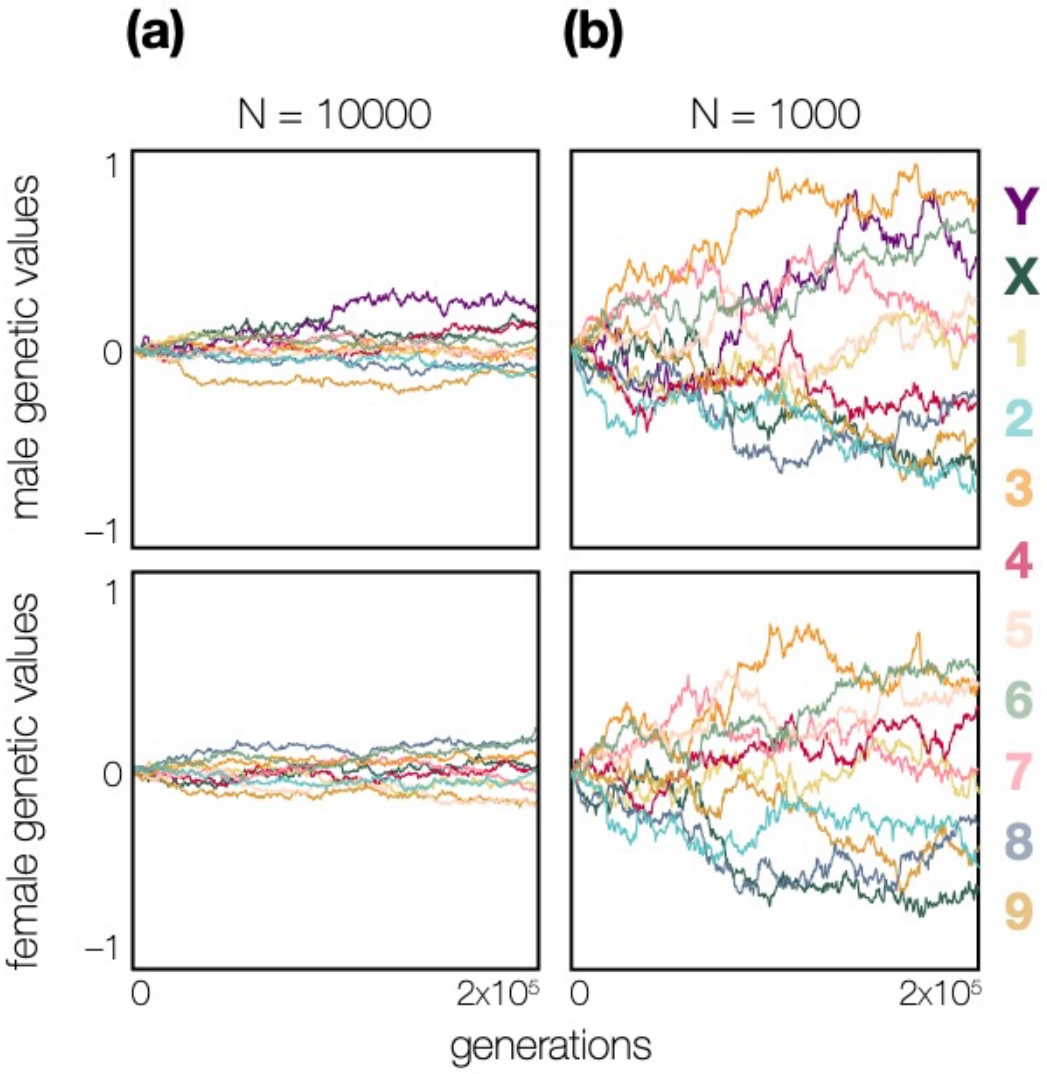

Fig. S5 | Chromosome-specific drift occurs more rapidly in smaller populations. Parameters are as in Fig. 1 in panel (a), but the population size is reduced to N = 1000 in panel (b). Results shown in each panel are from a single simulation run. Because drift is faster in smaller populations, the divergence in chromosomal values is correspondingly faster, driving the increased barriers to invasion in smaller populations shown in Fig. S4.

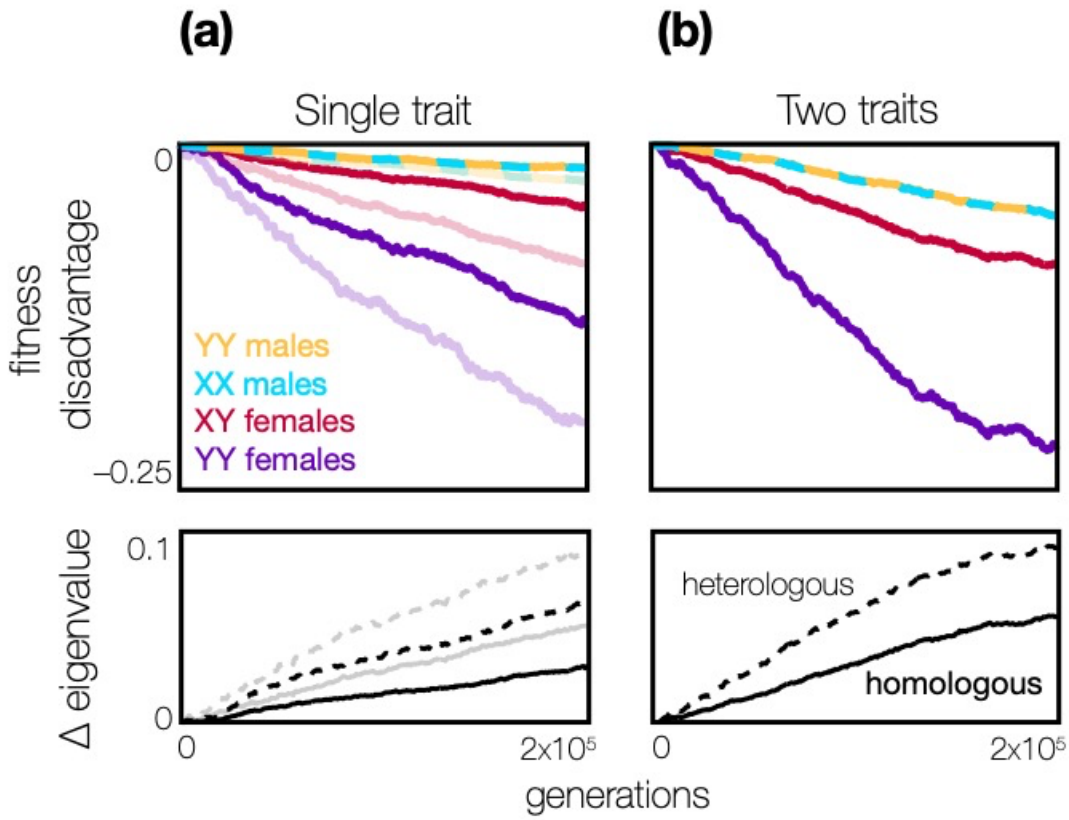

Fig. S6 | The existence of multiple traits under stabilizing selection enhances the barrier to sex chromosome turnover. The bold lines in (a) correspond to the scenario displayed in Fig. 2 of the main text, in which a single polygenic trait is encoded by 1000 loci and experiences stabilizing selection under a Gaussian fitness function of width $\sqrt{V_s} = 1$. The faded lines show the analogous scenario in which the strength of stabilizing selection is doubled ($\sqrt{V_s} = 0.5$). Panel (b) shows the fitness reductions to novel sexual genotypes in the scenario where two polygenic traits experience the same strength of stabilizing selection ($\sqrt{V_s} = 1$) and are independently affected by the same 1000 loci (or, equivalently, by 1000 sets of tightly linked loci). The consequences for sex chromosome turnover of having two traits, rather than one, under stabilizing selection are approximately the same as doubling the strength of selection on a single trait. Given the prevalence of stabilizing selection on polygenic phenotypes, the compounding selective disadvantages arising from multiple traits under selection are likely to be a significant factor promoting barriers to sex chromosome turnover.

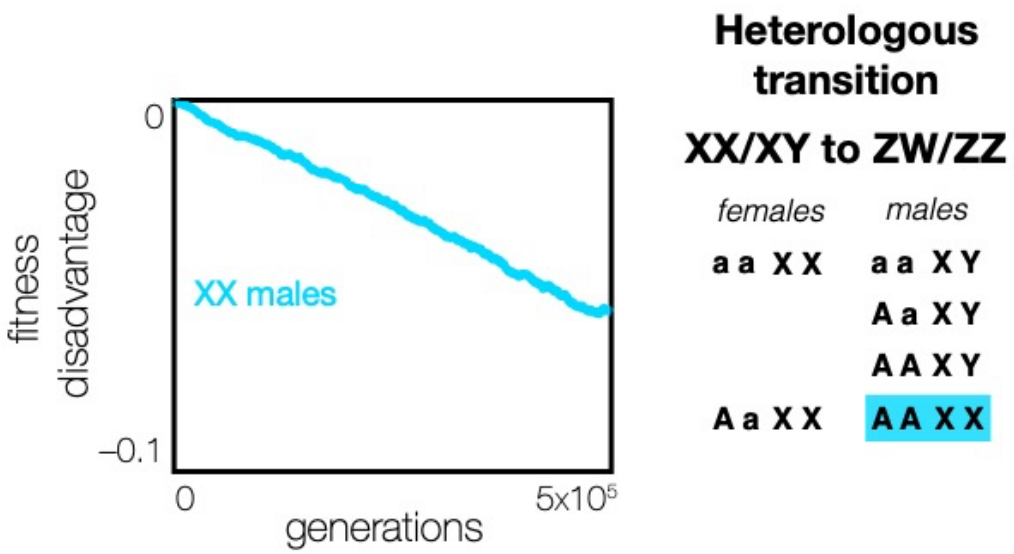

Fig. S7 | Heterogametic transitions that do not involve the creation of YY individuals are nonetheless impeded due to chromosome-specific drift. The scenario is as in Fig. 2b, but here a recessive heterologous transition in heterogamety is shown (rather than a dominant heterologous transition in heterogamety, as in Fig. 2b). This turnover is an example of a transition in sex determination that does not involve the production of YY individuals, and therefore would not be impeded by the exposure of deleterious recessive mutations that have accumulated on the Y chromosome. However, recessive heterologous turnovers are still impeded under the theory presented here, because novel sexual genotypes, which disrupt interchromosomal co-evolution, are necessarily produced in such turnovers.

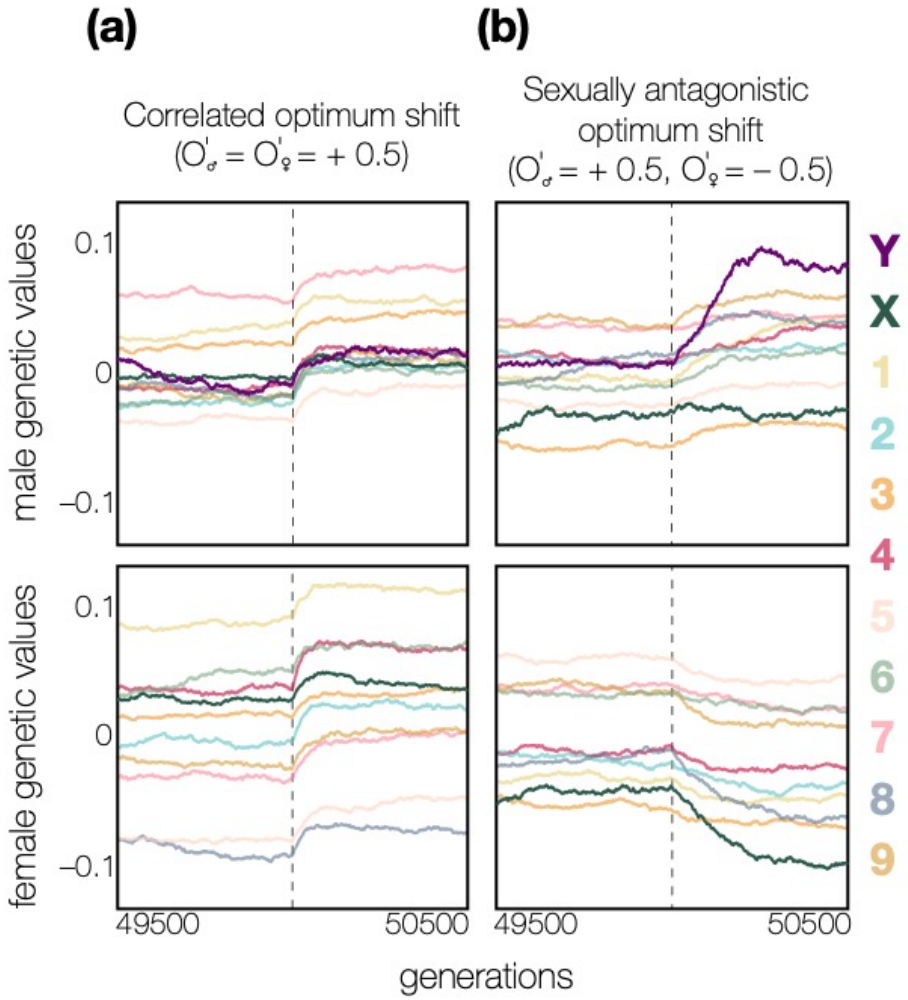

Fig. S8 | The X and Y chromosomes respond uniquely to a sexually antagonistic shift in male and female fitness optima. Each line represents the genetic value of a chromosome in a single simulation run. (a) In response to a concordant shift in the fitness optima, the mean values of all chromosomes, including the X and Y, shift in concert to move the male and female phenotype to the new, increased optimal value. (b) In response to a sexually antagonistic shift in the fitness optima, the mean genetic values of the X and Y chromosomes change disproportionately in opposite directions to facilitate the evolution of, respectively, females and males to their new divergent fitness optima.

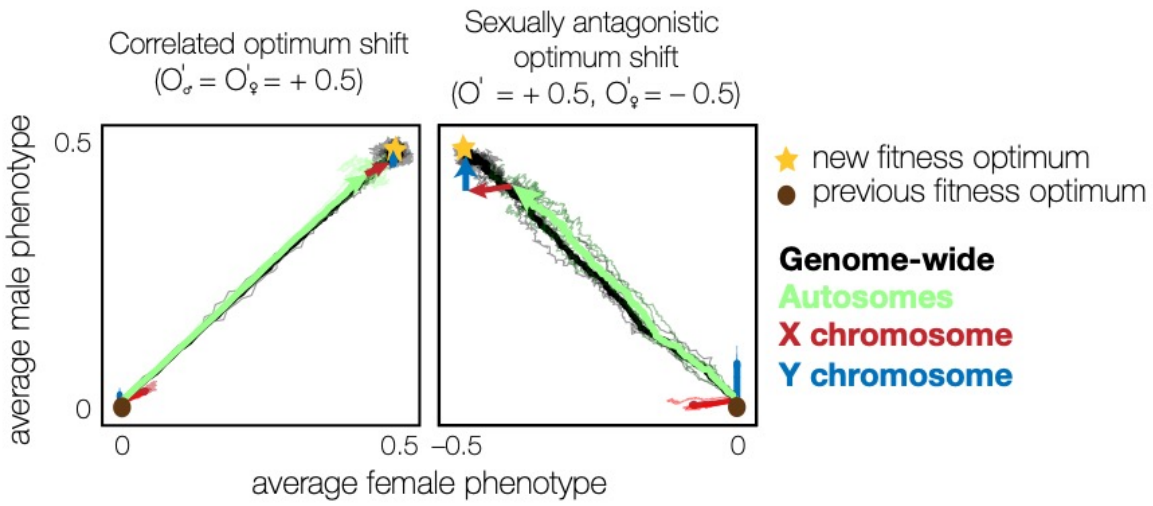

Fig. S9 | The sex chromosomes contribute disproportionately to the evolution of sexual dimorphism in quantitative traits. The phenotypic response to selection is shown on the male–female phenotypic landscape after a sexually antagonistic shift (left) and a correlated shift (right) in the fitness optimum. All parameters are the same as in Fig. 3. The brown circle marks the original fitness optimum, while the yellow star marks the new fitness optimum. Each faint line represents a single replicate (5 in total), in which phenotypes were recorded every generation for 500 generations following the shift in optimum; bold lines represent the average trajectory across those 5 replicates. Trajectories are normalized relative to their values at the time of the shift in optimum, so that all trajectories start at (0,0) in male–female phenotype space. The female genetic values for the trajectory of the Y chromosome are constrained to 0 for illustration, because the Y will not normally contribute to phenotypic evolution in females in an XX/XY sex chromosome system.

While overall phenotypic evolution (black) to the new optimum follows a straightforward trajectory in response to both shifts, the X (red) and Y (blue) chromosomes show nearly sex-specific contributions to phenotypic evolution after a sexually antagonistic shift, in striking contrast to their concordant behavior after a correlated shift. This disproportionate contribution of the sex chromosomes to phenotypic evolution under sexually antagonistic selection drives the increase in fitness costs associated with novel sexual genotypes after a sexually antagonistic shift, as shown in Fig. 3.

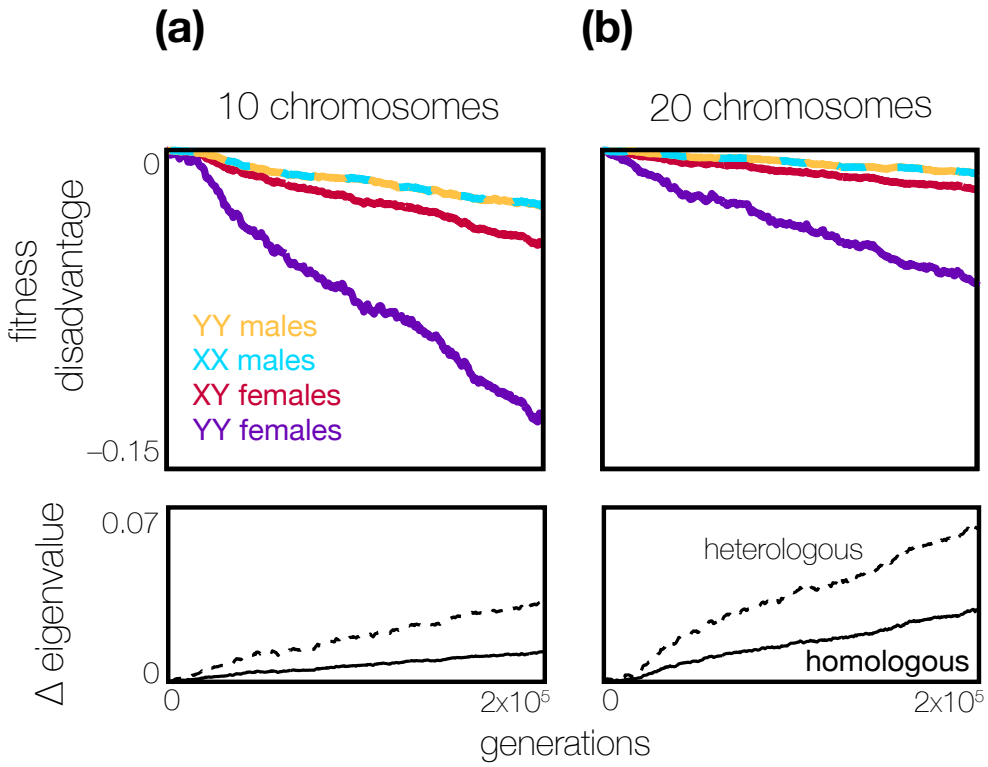

Fig. S10 | The size of sex chromosomes affects their long-term stability. Parameters are as in Fig. 2, but the 1000 genes underlying the quantitative trait are divided across (a) 10 (as in Fig. 2) or (b) 20 evenly sized chromosomes. If the sex chromosomes are a greater fraction of the genome, their mean values can drift more rapidly under stabilizing selection (SI Section S1) and they have a proportionally greater effect on the total phenotype; thus any rearrangements involving these chromosomes will be associated with greater fitness consequences.

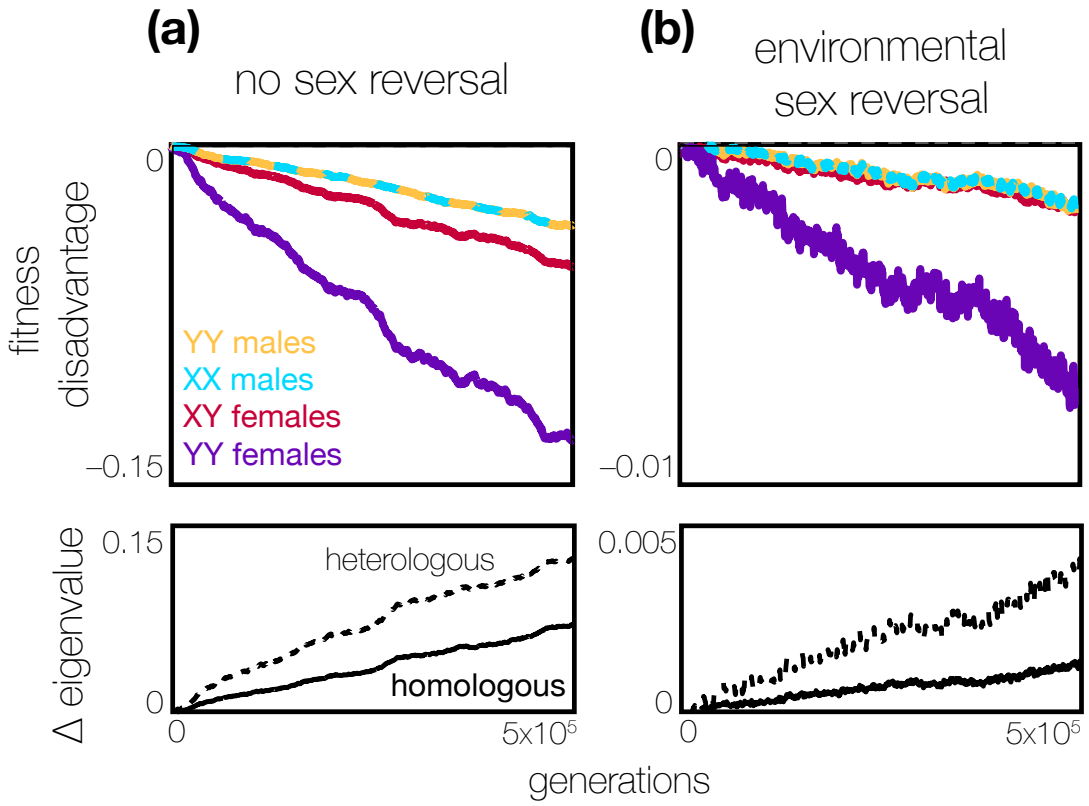

Fig. S11 | Environmental sex reversal enables sex chromosome turnovers across extended time scales. Parameters in panel (a) are as in Fig. 2, but a 1% rate of environmental sex reversal is implemented in panel (b), such that 1% of adult individuals have a phenotypic sex which is discordant with their genotypic sex. This sex reversal facilitates occasional recombination between the X and Y in XY females, whose recombination pattern is based on phenotypic, rather than genotypic, sex (Rodrigues et al. 2018, Perrin 2021). This occasional recombination facilitates a much greater agreement in genetic values between the sex chromosomes, which in turn slows the accumulation of fitness costs associated with novel sexual genotypes and thus greatly prolongs the period during which a sex chromosome turnover is possible. Note that, for visual clarity, panels (a) and (b) have different y-axes.